Proceedings of the ASME 2024 Conference on Smart Materials,
Adaptive Structures and Intelligent Systems
SMASIS2024
September 9-11, 2024, Atlanta, Georgia

# SMASIS2024-140167

# TOWARDS COMPLEX SHAPE ACTUATION: AN INVESTIGATION OF LOCAL AND GLOBAL MAGNETOACTIVE GRADIENTS IN 3D-PRINTED MULTI-STIMULI RESPONSIVE SHAPE MEMORY POLYMER COMPOSITES

#### Mohammad Hossein Zamani, Daniel Strobel, Zoubeida Ounaies

Electroactive Materials Characterization Lab, Mechanical Engineering Department, College of Engineering, Penn State University, University Park, PA, USA

#### **ABSTRACT**

In this research, we investigate multi-stimuli responsive multimaterial structures by combining shape memory polymers (SMPs) with magnetoactive fillers. Our objective is to design 3D-printed composites with local and global magnetoactive filler gradients, which exhibit complex shape actuation under magnetic and thermal fields. We first carry out a rheological study of SMP dispersions containing surface-treated magnetic particles to understand the effect of magnetic particle surface treatment, additives content, and shear rate on the complex flow behavior. Our findings reveal that dispersions filled with surface-treated magnetic particles exhibit enhanced shear thinning behavior and shape integrity compared to unfunctionalized dispersions. The improved rheological behavior and shape integrity are important results that indicate that PEG-functionalized SMP composites are promising candidates for direct ink printing. To create complex actuation, a 3D printing system is designed in a way that the magnetic particle-SMP dispersions are oriented using both shear and an external magnetic field, enabling a local angular gradient of magnetic particles. In addition, a global gradient is designed-in by varying the volume fraction of magnetic particles in the SMP suspensions. By adjusting the local and global gradients of magnetic particles within the SMP, different actuation patterns can be achieved. SEM analysis confirms the presence of the global gradient in iron oxide particles and their alignment along the magnetic field direction post-printing. Vibrating Sample Magnetometry (VSM) studies reveal an improved mass magnetization along the length of the printed samples, moving away from the printing origin. In addition, the iron oxide weight percent in the samples increases from 2.5 wt.% at the printing origin to 12.5wt.% at the end, creating a pronounced Fe<sub>3</sub>O<sub>4</sub> global gradient. These findings contribute to the development of advanced stimuli-responsive materials with tunable properties for various applications where complex shape actuation is required, including soft robotics, and biomedical devices.

Keywords: Rheology, 3D-printing, shape memory polymer, magnetic properties, iron oxide

#### 1. INTRODUCTION

Over the last few years, shape memory polymers (SMPs) have gained significant interest due to their unique functionality and properties. SMPs are widely epoxy-based due to their excellent mechanical properties and strong chemical resistance [1]. SMPs experience significant changes in stiffness and are able to return to their "remembered" shape when exposed to a stimulus, most often a change in temperature [2][3][4]. To achieve shape memory effect, a thermally actuated SMP can be brought above its glass transition temperature, fixed into a temporary shape, and cooled to lock in place. Then when the SMP is brought back above its glass transition temperature it returns to its original "remembered" shape without external forcing [5]. To achieve a multi-stimuli responsive composite, the SMPs can be filled with magnetoactive particles. When an external magnetic field is applied, the embedded magnetic particles can deform the polymer mechanically as they attempt to align with the external magnetic field [6]. The polymers filled with magnetoactive particles are referred to as magnetoactive SMPs and are manipulated by external thermal and magnetic stimuli. Magnetoactive SMPs with programable properties have gained significant interest as versatile candidates for biomedical applications due to their actuation capabilities, shape memory effect, and sensing capabilities [7].

Iron oxide (Fe<sub>3</sub>O<sub>4</sub>) has a wide range of applications due to its magnetic and functional properties. Fe<sub>3</sub>O<sub>4</sub> microparticles function as superparamagnetic materials. Superparamagnetic materials have no remnant magnetization meaning no magnetization occurs when an external magnetic field is removed [8]. Such magnetic particles can be classified as soft magnets. When exposed to an external magnetic field, the Fe<sub>3</sub>O<sub>4</sub> microparticles are magnetized and rapidly align with the external field due to their high magnetic susceptibility. The quick and

strong response to external magnetic fields and the ease to obtain Fe<sub>3</sub>O<sub>4</sub> particles make them great candidates for many applications such as magnetic resonance imaging, biological detection, and biomedical uses [9], [10].

The actuation patterns of magnetoactive SMPs are governed by the localization, orientation, and volume fraction of magnetic particles embedded within the polymer matrix. This research aims to design and fabricate a magneto-active SMP composite using Direct Ink Writing (DIW) and featuring both global and local Fe<sub>3</sub>O<sub>4</sub> gradients to achieve different actuation patterns. Here "global gradient" refers to the deliberate variation of Fe<sub>3</sub>O<sub>4</sub> volume content from the start to the end of print. "Local gradient" refers to the intentional orientation of Fe<sub>3</sub>O<sub>4</sub> within the polymer matrix. Attempting to develop such SMP composite requires addressing processing challenges. Firstly, due to the high surface charge of Fe<sub>3</sub>O<sub>4</sub> particles which leads to agglomeration, surface modification is imperative to achieve a composite with uniform dispersion and distribution of Fe<sub>3</sub>O<sub>4</sub> particles. Secondly, the continuous increase in the weight percentage of Fe<sub>3</sub>O<sub>4</sub> particles throughout the 3D printing process alters the rheology of the SMP inks dynamically. Therefore, to ensure a uniform print the composition of SMP inks must be tailored in a way that the rheological properties and shear thinning behavior of SMP inks remain as close as possible across varying Fe<sub>3</sub>O<sub>4</sub> concentrations. The study also explores the operating shear rate window in which the rheological properties of the SMP inks are relatively the same as each other despite the change in SMP composition. Thirdly, achieving a local gradient of Fe<sub>3</sub>O<sub>4</sub> within the SMP necessitates the design of a 3D printer capable of extruding the SMP ink through a magnetic field, subsequently locking the Fe<sub>3</sub>O<sub>4</sub> chaining post-exposure due to the soft magnetic properties of Fe<sub>3</sub>O<sub>4</sub> particles. To secure the Fe<sub>3</sub>O<sub>4</sub> particles in place, the printer must be engineered to facilitate the mixing of the crosslinking agent with the SMP composite immediately upon exiting the magnetic field. Lastly, this research characterizes the magnetic properties, magnetic particle weight percent, and the Fe<sub>3</sub>O<sub>4</sub> localization and chaining over the printed composite to assess our approach. The outcomes of this research contribute to our understanding of multi stimuliresponsive materials, especially those designed for 3D printing to exhibit structural anisotropy for controlled shape actuation.

# 2. MATERIALS AND METHODS

#### 2.1 Materials

In this research, epoxy resin (EPON 8111, Hexion Inc. ®) was used as the matrix and an aliphatic amine as the curing agent (EPIKURE 3271, Hexion Inc. ®). Magnetic particles (Fe<sub>3</sub>O<sub>4</sub>) with a diameter of 1-5 µm and 99.9% purity were purchased from Atlantic Equipment Engineers. Low molecular weight polyethylene glycol400 (Alfa Aesar) was utilized for magnetic particle surface treatment. Fumed silica (99% purity, McMaster-CARR) was used as the rheology modifier.

#### 2.1.1 Iron Oxide Functionalization

To coat a layer of polyethylene glycol on the surface of the magnetic particles, 1 g of Fe<sub>3</sub>O<sub>4</sub> was combined with 30 ml of deionized water. This mixture underwent ultrasonication using a 750-watt ultrasonic homogenizer (Cole-Parmer, Vernon Hills, IL) for 5 minutes at 40% amplitude, aiming to disperse any particle clusters. Following this, the Fe<sub>3</sub>O<sub>4</sub> particles were isolated and reserved for later use. Subsequently, 9 g of polyethylene glycol (PEG) was dissolved in 21 g of deionized water to create 30 wt.% of PEG aqueous solution. The solution was then homogenized using a magnetic stirrer at 80°C and a stirring speed of 200 rpm for 20 minutes. Once cooled to ambient temperature, the Fe<sub>3</sub>O<sub>4</sub> particles were added to PEG solution. For thorough mixing of the Fe<sub>3</sub>O<sub>4</sub>-PEG dispersion, a mechanical stirrer operated for 1 hour at room temperature with a speed of 200 rpm. This was succeeded by a centrifugation step for 3 minutes at 10,000 rpm using an Allegra X-30 Centrifuge (Beckman Coulter, Indianapolis, IN) to separate the PEGfunctionalized Fe<sub>3</sub>O<sub>4</sub> particles from the dispersion. The separated particles were then washed twice with deionized water to remove surplus PEG and centrifuged again under the same conditions. Post-washing, the particles were dried in an oven at 80°C for 2 hours. The functionalized Fe<sub>3</sub>O<sub>4</sub> particles were then stored for ink preparation.

#### 2.1.2 Ink Preparation

Three SMP inks with different compositions of epoxy, fumed silica, and surface treated Fe<sub>3</sub>O<sub>4</sub> were prepared (see Table 1). Initially, the epoxy resin was combined with fumed silica. Following this, Fe<sub>3</sub>O<sub>4</sub> microparticles were incorporated into the mixtures. To eliminate any clusters, each sample underwent a sonication process for 5 minutes at 40% amplitude.

Table 1. Composition of SMP Silica Fe<sub>3</sub>O<sub>4</sub> PEG30 Inks

Sample nomenclature	Epoxy wt.%	Fumed Silica wt.%	Fe <sub>3</sub> O <sub>4</sub> wt.%
SMP(94.85)-Silica(2.65)-Fe <sub>3</sub> O <sub>4</sub> (2.5)-PEG30	94.85	2.65	2.5
SMP(90.99)-Silica(1.51)-Fe <sub>3</sub> O <sub>4</sub> (7.5)- PEG30	90.99	1.51	7.5
SMP(86.37)-Silica(1.13)-Fe3O4(12.5)- PEG30	86.37	1.13	12.5

#### 2.2 3D-Printing of SMP Inks

To achieve local-angular and global gradient of magnetic particles within the printed layer, a specific 3D-printing setup was designed. To control the printing process, we programmed the 3D-printer with a g-code file to print a 50×150×2.5 ml cube. The 3D-printing design schematic is shown in Figure 1. First, we loaded SMP\_Silica\_Fe<sub>3</sub>O<sub>4</sub>\_PEG30 inks into the printer's syringe. The inks were designed such that the weight percentage of Fe<sub>3</sub>O<sub>4</sub> magnetic particles linearly increased from 2.5 wt.% at the syringe tip to 12.5 wt.% at the base, ensuring a controlled gradient in magnetic particle concentration throughout the printed object. The operational mechanism of our system relied on the precise delivery of the SMP inks at a flow rate of 1.61 ml/min through a magnetic field generated by an 3.5A close

circuit. A magnetic shield was placed beneath the field to prevent any unintended magnetic influence on the non-targeted sections of the ink stream. To lock the magnetic particles' orientation as well as localization within the polymer matrix, a stream of EPIKURE curing agent was concurrently administered at a flow rate of 0.9 ml/min using a syringe pump. This stream blended with the SMP ink immediately after exiting the magnetic field zone. The resultant mixture was then deposited onto the build platform through a robotically controlled extrusion nozzle with a quarter-inch diameter.

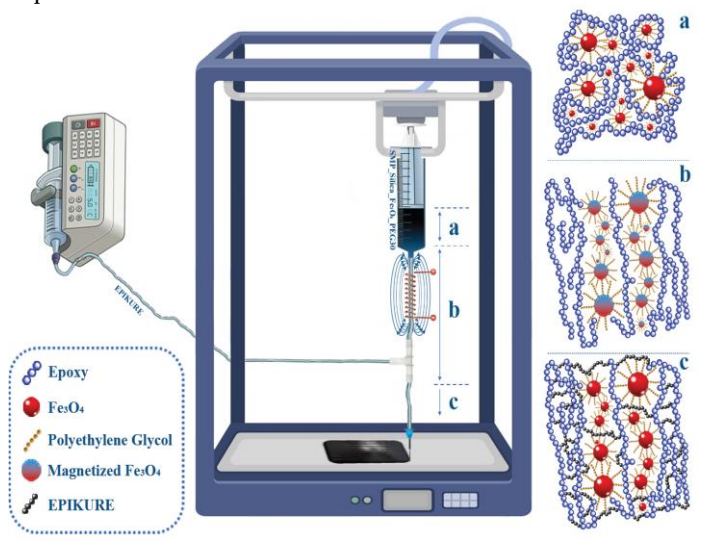


Figure 1. 3D-printing process of SMP schematic: Dispersed Fe<sub>3</sub>O<sub>4</sub> particles in random coil epoxy resin (a), Fe<sub>3</sub>O<sub>4</sub> chains formed under the magnetic field within shear-induced elongated epoxy resin chains (b), and Fe<sub>3</sub>O<sub>4</sub> locked chains within the crosslinked epoxy matrix (c)

# 2.3 Characterization Tests

#### 2.3.1 Particle Dispersions

In order to study the morphology and magnetic particle dispersion in the composite, a Verios G4 scanning electron microscope was used for imaging of the planar surface of the composite. A layer of iridium was sputtered on the surface of the composite before conducting the micrography.

#### 2.3.2 Magnetic Characterization

The magnetic properties of the SMP composites were assessed using a Vibrating Sample Magnetometer (VSM) (MicroSense LLC, Lowell, Massachusetts). This advanced technique allows for the precise measurement of a material's magnetic response by vibrating the sample within a uniform magnetic field and detecting the induced electrical current in surrounding precision coils. The vibrational motion of the magnetic material in the magnetic field generates an electrical induction, which is captured by large coils to determine the material's magnetization across varying magnetic field strengths. Through this process, we are able to construct magnetic hysteresis loops for our samples, providing invaluable insights into their magnetic

behaviors. The VSM test was performed on each sample in both in-plane and out-of-plane orientations. This dual-mode approach was employed to assess any anisotropic characteristics within the composite's structure, ensuring a thorough understanding of its directional magnetic properties.

### 2.3.3 Rheology

Rheological study of SMP inks was conducted using a rotary viscometer (IKA Rotavisc hi-vi, Wilmington, Measurements were conducted over a shear rate range from 10 to 200 s<sup>-1</sup>, employing a VOL-SP-6.7 spindle at ambient temperature. The power law equation (Equation (1)) was then employed on the results to understand the complex flow behavior under shear stress.

$$\tau = k\dot{\gamma}^n \tag{1}$$

Where  $\tau$  is shear stress (Pa)  $\dot{\gamma}$  is shear rate (s<sup>-1</sup>), k is power law consistency constant (Pa. $s^n$ ), and n is power-law index. Also, based on the formula of the viscosity of a dispersion (Equation (2)), Equation (3) can be used to study the rheological behavior of SMP inks under shear stress.

$$\eta = \frac{\tau}{\dot{\gamma}}$$

$$\eta = k\dot{\gamma}^{1-n}$$
(2)
(3)

$$\eta = k\dot{\gamma}^{1-n} \tag{3}$$

#### 2.3.4 Velocity Profile of Non-Newtonian Flow

To determine the 3D-printing window where the rheological behavior of different compositions of SMP inks is relatively the same as each other, the velocity profile of a non-Newtonian pressure driven laminar fluid flow in a tube (see Figure 2) was derived. Considering the forces acting on the fluid in the pipe, based on Cauchi momentum equation (Equation (4)), it may be shown that:

$$\rho \frac{du}{dt} = \nabla \cdot \sigma + f \tag{4}$$

Where  $\rho$  is density of the fluid, u is the flow velocity, t is time,  $\sigma$  is the Cauchy stress tensor, and f accounts for body forces present [11].

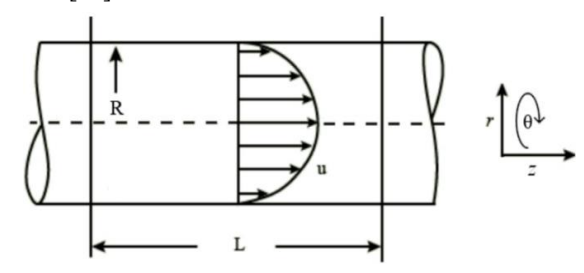


Figure 2. The velocity profile schematic of a non-Newtonian pressure driven laminar fluid flow in a tube

15

# 3. RESULTS AND DISCUSSION

# 3.1 Rheology

Rheological properties are crucial to describing the behavior of inks in direct ink writing. As the weight percent of Fe<sub>3</sub>O<sub>4</sub> increases over the 3D-printing process, the viscosity and shear thinning behavior of SMP inks change continuously. This means that, in order to achieve a uniform print, either the flow rate needs to be adjusted very quickly, or the rheology of the inks should be engineered in a way that increasing the weight percent of Fe<sub>3</sub>O<sub>4</sub>, maintains the same rheology characteristics, regardless of the relative content of the constituents in the ink. We first conducted comprehensive rheological study SMP Silica Fe<sub>3</sub>O<sub>4</sub> PEG30 inks to understand the effect of ink composition, magnetic particle surface treatment, and the shear rate on the viscosity and flow behavior. After meticulous data analysis of 41 data sets, we developed an empirical equation (see Equation (5) that can anticipate the power law index (n) value as a function of the fumed silica volume fraction ( $v_1$ ) and Fe<sub>3</sub>O<sub>4</sub> volume fraction  $(v_2)$ .

$$n = -2.0193(1.93v_1^{0.1} + v_2^{0.5}) + 4.0494$$
 (5)  
,  $R^2 \approx 0.99$ 

we then set the power law index values to 0.6, and calculated the volume fraction of the constituents to create SMP inks loaded with 2.5, 5, 7.5, 10, 12.5, and 15 wt.% Fe<sub>3</sub>O<sub>4</sub>. As can be seen in Figure 3a, the viscosity decreases with increasing shear rate. This behavior means that all the SMP inks exhibit shear thinning behavior, which is vital for successful direct ink writing [12]. In particular, within the moderate regime where the shear rate is below 30 1/s, the viscosity difference in all samples is less than 4.5 Pa.s; this difference in the viscosity for the various SMP compositions at each shear rate is relatively small and it is unlikely to cause issues to the uniformity of the print. Moreover, with the incremental increase in Fe<sub>3</sub>O<sub>4</sub> volume content across zones—but still under 2.5 wt.%—the viscosity change is minimal, not exceeding 1 Pa.s. Figure 3b shows the power law index and power law constant as a function of Fe<sub>3</sub>O<sub>4</sub> and fumed silica wt%. The power law constant, which is an indication of the level of shear thinning behavior of the flow, is in the range of 0.56 to 0.72 [13]. It means that increasing the Fe<sub>3</sub>O<sub>4</sub> loading does not affect the level of shear thinning behavior. Moreover, the power law constant, which represents the flow consistency, or in other words the shape integrity of the resin after deposition, is in the range of 9 and 16 for all samples [14]. Considering the low difference in viscosity magnitudes of SMP inks with different compositions at all shear rates, and relatively similar power law index and power law constant values, the rheological properties of the SMP inks will be relatively the same as each other over the 3D-printing process. According to Figure 3a, at 39 1/s, the viscosity of SMP(94.85) Silica(2.65) Fe<sub>3</sub>O<sub>4</sub>(2.5) PEG30 and SMP(9314) Silica(1.86) Fe<sub>3</sub>O<sub>4</sub>(5) PEG30 see a decrease of 1 Pa.s.; at this high shear rate, this change may introduce complications and may merit further consideration when

processing. To ensure no such issue happens during the 3D-printing, we define an operating window in which the rheological properties are the same and linear logarithmic shear thinning behavior takes place. To find the upper limit of the operating window, we need to derive the velocity profile of a power law pressure driven pipe flow using Equation (4). Based on the g-code we used to program the 3D-printing process, the printer begins moving after 1 minute of depositing SMP inks to reach steady state. As for the modeling assumptions we consider steady state, axisymmetric flow behavior, unidirectional flow, and fully developed flow. Now Equation (4) can be written as follows (Equation (6)):

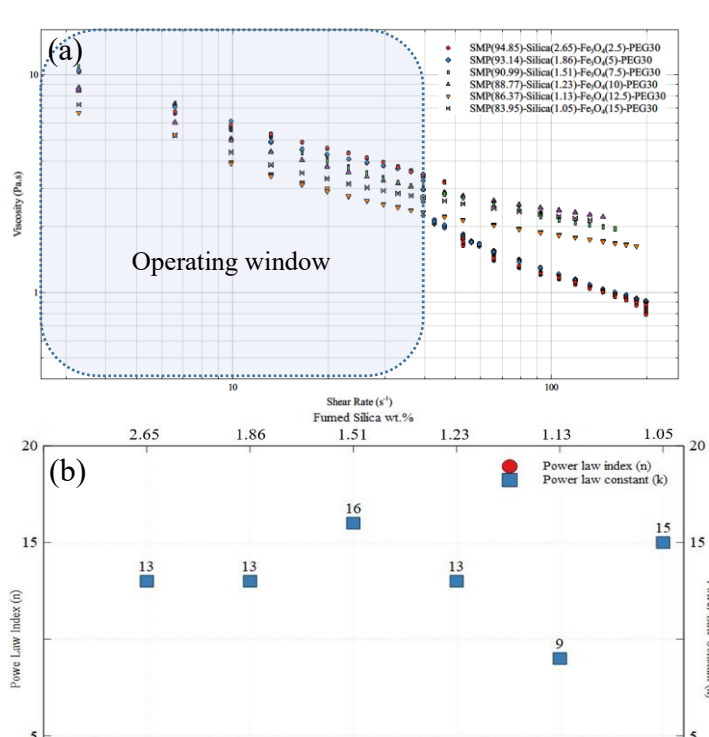


Figure 3. Viscosity versus shear rate (a) and power law index and power law constant as a function of  $Fe_3O_4$  and fumed silica wt.% (b) for SMP inks

Fe<sub>2</sub>O<sub>4</sub> wt.%

$$\rho \left[ \frac{\partial u_{z}}{\partial t} + u_{r} \frac{\partial u_{z}}{\partial r} + \frac{u_{\theta}}{r} \frac{\partial u_{z}}{\partial \theta} + u_{z} \frac{\partial u_{z}}{\partial z} \right] =$$

$$- \frac{\partial P}{\partial z} + \left[ \frac{1}{r} \frac{\partial}{\partial r} (r \tau_{rz}) + \frac{1}{r} \frac{\partial}{\partial \theta} (\tau_{\theta z}) + \frac{\partial \tau_{zz}}{\partial z} \right]$$

$$\tau_{rz} = k \left( \frac{\partial u_{z}}{\partial r} \right)^{n}$$

$$(7)$$

Boundary conditions: @  $r = R \rightarrow u_z = 0$ ,  $u_z \neq \infty$  We can then solve the Cauchi momentum equation for SMP inks:

$$u_z(r) = \frac{n}{n+1} \left(\frac{R^{n+1}\Delta P}{2kL}\right)^{\frac{1}{n}} \left(1 - \left(\frac{r}{R}\right)^{\frac{n+1}{n}}\right) \tag{8}$$

Where  $u_z(r)$  is the velocity profile of SMP inks with power law index n and power law constant k in a tube with radius of R, length of L, and pressure difference of  $\Delta P$ . Now, we can derive the flow rate from Equation (8):

$$Q = \int_0^L u_z dA = \frac{n\pi R^3}{3n+1} \left(\frac{R\Delta P}{2kL}\right)^{\frac{1}{n}}$$
(9)

The shear stress on the wall can be calculated using Equation (10):

$$\tau_{\rm w} = \frac{{\rm R}\Delta P}{2{\rm L}} \tag{10}$$

To define the upper limit of the operating window, we consider the  $39.59 \text{ s}^{-1}$  as the maximum shear rate. At this shear rate, the shear stress is 137.87 Pa. Also, we know that the maximum shear stress on the fluid is on the walls [15]. So, the maximum shear rate can be calculated by Equation (11):

$$Q_{max} = \frac{n\pi R^3}{3n+1} (\tau_{max})^{\frac{1}{n}}$$
 (11)

Considering SMP(93.14)\_Silica(1.86)\_Fe<sub>3</sub>O<sub>4</sub>(5)\_PEG30 rheological constants and the radius of the tube to be a quarter inch, the maximum flow rate below which the rheological properties are relatively the same is 930.366 ml.min<sup>-1</sup>. Based on the fact that we print at 2.56 ml.min<sup>-1</sup>, we are well within the operating window shown in Fig. 3a.

In summary, the rheological properties of the SMP\_Silica\_Fe<sub>3</sub>O<sub>4</sub>\_PEG mixtures remain consistent across varying Fe<sub>3</sub>O<sub>4</sub> concentrations, by making rheological adjustments to the SMP\_Silica\_Fe<sub>3</sub>O<sub>4</sub>\_PEG30 mixtures. This understanding of the rheological behavior allows us to maintain the viscosity variations to below 4.5 Pa.s, while the range of both the power law index and power law constant is between 0.56-0.72 and 9-16, respectively. Modeling the flow behavior of this non-Newtonian fluid within a tube confirms that the rheological characteristics of the inks remain stable under flow rate of 930 ml/s.

# 3.2 Magnetic Properties

To investigate the global gradient of SMP composites we define seven zones as illustrated in Figure 4. Then VSM tests were conducted on samples from each zone to investigate their magnetic properties. Figure 5a shows the magnetic hysteresis loops of different zones of SMP composite printed without a magnetic field. The hysteresis loops all cross the x-axis at zero

which confirms that the Fe<sub>3</sub>O<sub>4</sub> microparticles have no remnant magnetization and are soft magnetic materials [16].

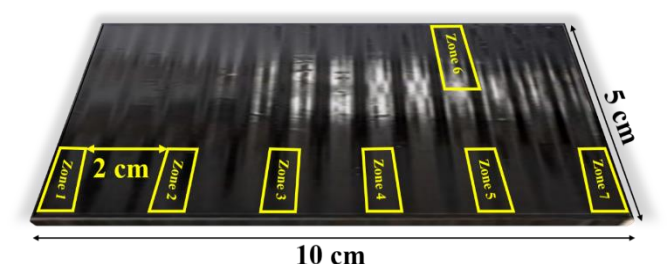
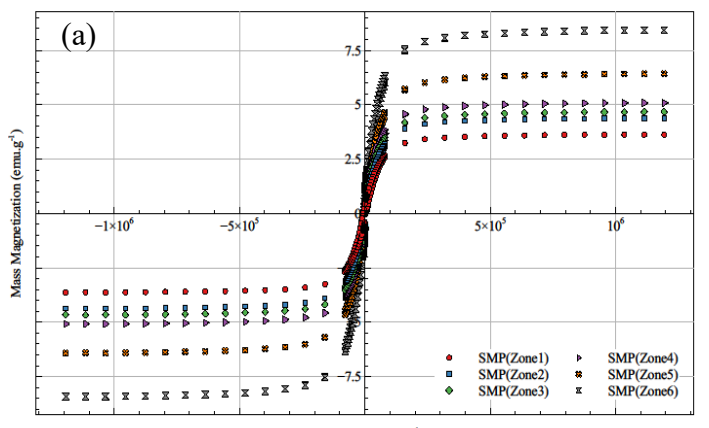


Figure 4. 5cm×10 cm SMP divided into seven zones where the print starts from zone1 (origin) and ends at zone7

In Figure 5a, the y-axis represents the magnetic flux density, or strength of magnetic field within the SMPs. The maximum magnetic flux densities of all zones occur with the highest external field applied as expected. It can be seen that the maximum magnetic flux density increases across each zone with zone1 having the lowest and zone7 having the largest. These results correspond to the global gradient across the printed samples with zone1 having the lowest weight percentage of Fe<sub>3</sub>O<sub>4</sub> at 4.98% and zone7 having the highest weight percentage of Fe<sub>3</sub>O<sub>4</sub> at 11.46%, as shown in Figure 5b.



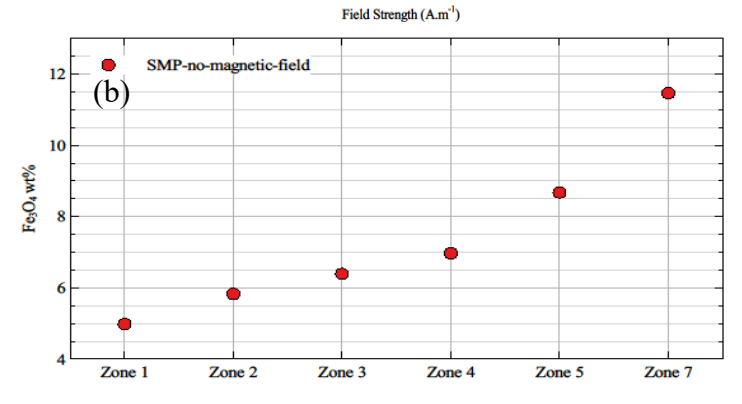


Figure 5. Hysteresis loops of different SMP zones (a) and Fe<sub>3</sub>O<sub>4</sub> weight percent of each SMP zone (b)

The varying magnetic flux densities indicates that the different zones will respond differently to applied external magnetic fields; i.e., once the composite is exposed to a uniform external magnetic field, the level of actuation of each zone will be different, enabling the composite to exhibit a more complex deformation. This approach can be applied in designing magneto-active SMPs to create complex actuation patterns by controlling the localization of magnetic particles in different locations of the polymer matrix.

#### 3.3 Iron Oxide Particles' Localization in SMP

SEM was conducted to investigate the  $Fe_3O_4$  particles' distribution within the polymer matrix. Figure 6 shows the SEM micrographs of SMP samples printed without magnetic field (H = 0). As can be seen in both Figure 6a and Figure 6b,  $Fe_3O_4$  are well dispersed within the matrix which is mostly due to the PEG surface treatment. Another notable observation is the higher volume content of  $Fe_3O_4$  in zone6 compared with zone5. This shows that the printing technique is effective at creating a global gradient along the printed magnetoactive SMP.

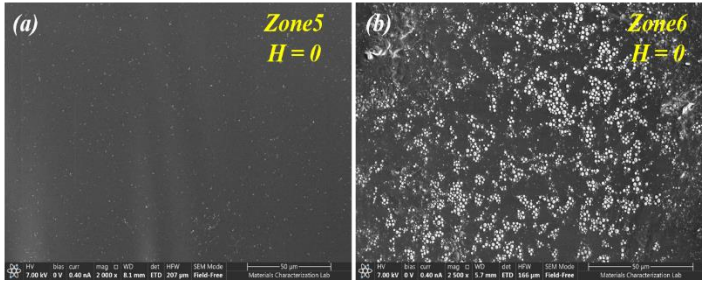


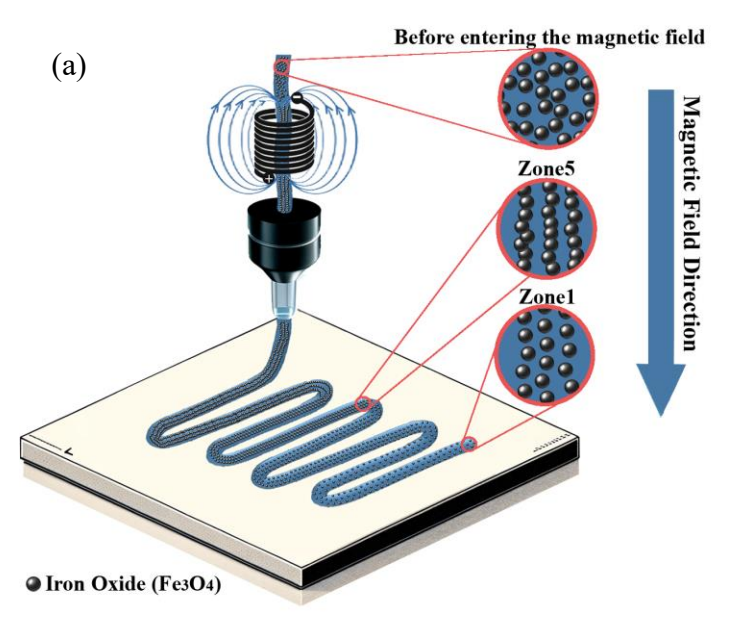
Figure 6. SEM micrographs of SPM zone5 (a) and zone6 (b) 3D printed without magnetic field (H = 0)

To determine whether the printing method is able to establish a local gradient of Fe<sub>3</sub>O<sub>4</sub>, SEM was conducted on SMP composite 3D printed under a magnetic field (See Figure 7). As illustrated in Figure 7a, Fe<sub>3</sub>O<sub>4</sub> microparticles form chains, with thin chains aligning along the path of printing, which is also the path of the applied magnetic field. Figure 7b and Figure 7c confirms the Fe<sub>3</sub>O<sub>4</sub> chain formation through the direction of the magnetic field. This local gradient proves the method of applying an external magnetic field via coiled copper wire is strong enough to locally align the Fe<sub>3</sub>O<sub>4</sub> microparticles.

#### 4. CONCLUSION

Surface modification of Fe<sub>3</sub>O<sub>4</sub> particles with polyethylene glycol (PEG) significantly enhances their dispersion within the epoxy matrix, resulting in a more homogeneous distribution of Fe<sub>3</sub>O<sub>4</sub> particles. Fumed silica plays an important role in the shear thinning behavior observed in the SMP\_Silica\_Fe<sub>3</sub>O<sub>4</sub>\_PEG30 inks. Notably, the rheological behavior of these inks remains consistent when flowing through a nozzle with a quarter-inch diameter at flow rates below 930 ml/min. Moreover, a controlled global gradient of Fe<sub>3</sub>O<sub>4</sub> particles has been successfully achieved, enabling the customization of material properties according to the requirements of the end-use application.

Additionally, by applying a magnetic field, a local gradient, or 'chaining', of  $Fe_3O_4$  is achieved. This novel approach of integrating both shear forces and magnetic fields paves the way for the development of materials with intricate and complex actuation patterns.



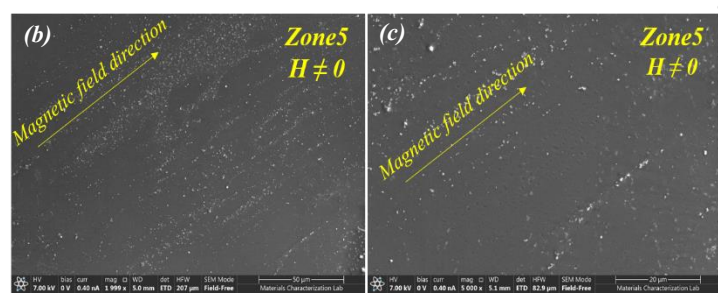


Figure 7. Schematic of 3D-printed SMP showing the local and global gradient of Fe3O4 (a) and SEM micrographs of SPM zone5 3D printed under magnetic field at two different magnifications (H  $\neq$  0) (b, c)

#### **ACKNOWLEDGEMENTS**

The authors would like to acknowledge support from the National Science Foundation under Grant No. NSF CMMI-2152984.

#### **REFERENCES**

- [1] Mousavi SR, Zamani MH, Estaji S, Tayouri MI, Arjmand M, Jafari SH, et al. Mechanical properties of bamboo fiber-reinforced polymer composites: a review of recent case studies. *J Mater Sci.* 2022;57(5):3143-3167. doi:10.1007/s10853-021-06854-6
- [2] Leng R, Uitz O, Ounaies Z, Seepersad C. Design and Characterization of a Multilayered Multifield-Actuated

- Polymer Unimorph. In: ASME 2021 Conference on Smart Materials, Adaptive Structures and Intelligent Systems. American Society of Mechanical Engineers; 2021. doi:10.1115/SMASIS2021-68238
- [3] Uitz O, Leng R, Pan T, Zhao X, Oridate A, Seepersad C, et al. Reactive extrusion additive manufacturing (REAM) of functionally graded, magneto-active thermoset composites. *Addit Manuf.* 2023;67:103486. doi:10.1016/j.addma.2023.103486
- [4] Pandey A, Singh G, Singh S, Jha K, Prakash C. 3D printed biodegradable functional temperature-stimuli shape memory polymer for customized scaffoldings. *J Mech Behav Biomed Mater*. 2020;108. doi:10.1016/j.jmbbm.2020.103781
- [5] Ze Q, Kuang X, Wu S, Wong J, Montgomery SM, Zhang R, et al. Magnetic Shape Memory Polymers with Integrated Multifunctional Shape Manipulation. *Advanced Materials*. 2020;32(4). doi:10.1002/adma.201906657
- [6] Bastola AK, Hossain M. The shape morphing performance of magnetoactive soft materials performance. *Mater Des.* 2021;211. doi:10.1016/j.matdes.2021.110172
- [7] van Vilsteren SJM, Yarmand H, Ghodrat S. Review of magnetic shape memory polymers and magnetic soft materials. *Magnetochemistry*. 2021;7(9). doi:10.3390/magnetochemistry7090123
- [8] Baumgartner J, Bertinetti L, Widdrat M, Hirt AM, Faivre D. Formation of Magnetite Nanoparticles at Low Temperature: From Superparamagnetic to Stable Single Domain Particles. *PLoS One*. 2013;8(3). doi:10.1371/journal.pone.0057070
- [9] Koo KN, Ismail AF, Othman MHD, Rahman MA, Sheng TZ. Preparation and characterization of superparamagnetic magnetite (Fe3O4) nanoparticles: A short review. *Malaysian Journal of Fundamental and Applied Sciences*. 2019;15(1). doi:10.11113/mjfas.v15n2019.1224
- [10] Xiao D, Lu T, Zeng R, Bi Y. Preparation and highlighted applications of magnetic microparticles and nanoparticles: a review on recent advances. *Microchimica Acta*. 2016;183(10). doi:10.1007/s00604-016-1928-y
- [11] Acheson DJ. *Elementary Fluid Dynamics*. Oxford University Press; 1990.
- [12] Rau DA, Williams CB, Bortner MJ. Rheology and printability: A survey of critical relationships for direct ink write materials design. *Prog Mater Sci.* Published online 2023:101188.
- [13] Picchi D, Poesio P, Ullmann A, Brauner N. Characteristics of stratified flows of Newtonian/non-Newtonian shear-thinning fluids. *International Journal of Multiphase Flow.* 2017;97:109-133.
- [14] Pang B, Wang S, Chen W, Hassan M, Lu H. Effects of flow behavior index and consistency coefficient on

- hydrodynamics of power-law fluids and particles in fluidized beds. *Powder Technol*. 2020;366:249-260.
- [15] Katritsis D, Kaiktsis L, Chaniotis A, Pantos J, Efstathopoulos EP, Marmarelis V. Wall shear stress: theoretical considerations and methods of measurement. *Prog Cardiovasc Dis.* 2007;49(5):307-329.
- [16] Riesgo G, Elbaile L, Moriche R, Carrizo J, Crespo RD, García MA, et al. Influence of the remnant magnetization, size distribution and content of soft magnetic reinforcement in micro-mechanical behavior of polymer matrix composites. *Polym Test*. 2019;79:106020.